Print ISSN 2710-0200 *Full text available online at* *Ethiop J Nat Comp Sci.*
Electronic ISSN 2710-0219 *http://journal.uog.edu.et/index.php/EJNCS* *Vol. 4 (1) 569-585*
https://doi.org/*10.20372/ejncs/Ma.2024.017*

ORIGINAL RESEARCH

Unraveling the Thermo-Physical Properties of MHD Heat and Mass Transfer of Nano-Fluid Flow over a Nonlinear Permeable Stretching Sheet

Idongesit F. Ekang[1*], Amos O. Popoola[2]

[1]Department of Mathematics, University of Uyo, Uyo, Nigeria
[2]Department of Mathematical Sciences, Osun State University, Osogbo, Nigeria
[*]Corresponding author: idongesitekang@uniuyo.edu.ng

Received: 9 March 2023 / Accepted: 2 July 2024 / Published: 29 August 2024

Abstract

Investigating MHD Heat and mass transfer of nano-fluid over a permeable stretching sheet can lead to improved storage, handling and usage. This work therefore examined the significance of temperature-dependent viscosity and temperature-dependent thermal conductivity on MHD heat and mass transfer of nano-fluid over a nonlinear permeable stretching sheet. The governing partial differential equations describing the nanofluid flow are transformed and parameterized into a system of ordinary differential equations. The resulting mathematical model was solved numerically using the shooting technique with the fourth-order Runge-Kutta method. Graphical analysis is conducted to investigate the impact of certain fluid parameters on the momentum, thermal and concentration equations. The results from the graphs showed that temperature-dependent viscosity and temperature-dependent thermal conductivity have appreciable effects on the model.

Keywords: Nano-fluid, MHD, temperature-dependent viscosity and temperature-dependent thermal conductivity, nonlinear stretching sheet

Introduction

The field of MHD heat and mass flow has received significant advancement within engineering and scientific processes in recent years. In particular, boundary layer flow over stretching sheets have played crucial roles in various technological applications such as paper production, hot rolling, glass-fibre production, and extraction of polymer sheets.

Sakkiadis (1961) first conducted pioneering work on boundary layer behaviour on continuous solid surfaces, while Crane (1970) analysed the flow past a stretching plate. Gupta and Gupta (1977) examined a stretching sheet with suction or blowing using the method of similar solutions. Vajravelu (2001), on the other hand, used numerical methods to investigate viscous flow over a nonlinearly stretching sheet and found that heat always flows from the stretching sheet to the fluid. Wang (2009) researched the effects of suction and surface slip on viscous flow on a stretching sheet.

Nano-fluids, which are fluids containing nano -particles with sizes less than 100nm, are of great importance in numerous heat transfer

processes, including petroleum refining, pharmaceuticals, engine cooling/ vehicle thermal management, chillers, fuel cells, domestics refrigerators, and grinding, among others. Common base fluids for nano-fluids include water, ethylene glycol, and various oils derived from conventional minerals oils, crude oil, and refined crude oil. It also exhibits unique optical, electrical, and rheological properties that can be tailored by adjusting the nanoparticle size, shape, and concentration.

Khan and Pop (2010) analysed the stretching sheet of a nano-fluid flow while Rana and Bhargava (2012) studied flow and heat transfer of a nano-fluid over a nonlinearly stretching sheet, through a numerical study. Das (2015) considered a nano-fluid flow with partial slip over a nonlinear permeable stretching sheet and found that an increase in the slip parameter and nonlinear stretching parameter leads to a decrease in the velocity of the nano-fluid.

Ekang *et al.* (2022) analysed Casson fluid flow with heat generation and radiation effect through a porous medium of an exponentially shrinking sheet.

Ayeni *et al.* (2009) investigated MHD flow and heat transfer of a viscous reacting fluid over a stretching sheet. Eid and Mahny (2017) conducted research on non-Newtonian nano-fluid of unsteady MHD transfer over a permeable stretching wall with heat generation/ absorption. Popoola *et al.* (2016) analysed heat and mass transfer on MHD viscoelastic fluid flow in the presence of thermal diffusion and chemical reaction. Senge *et al.* (2021) explained MHD flow over a stretching sheet in a thermally stratified porous medium. Oreyeni *et al.* (2022) studied the significant of exponential space-based heat generation and variable thermo-physical properties on the dynamics of Casson fluid over a stratified surface with non-uniform thickness. Oreyeni *et al.* (2022) analysed the impacts of stratification on an inclined hydromagnetic bioconvective flow of micropolar nano-fluid with exponential space-based heat generation. Ekang *et al.* (2021) examined MHD heat and mass flow of nano-fluid over a nonlinear permeable stretching sheet.

Temperature-dependent viscosity means that the viscosity of the fluid changes with temperature, which can affect the flow behaviour and the heat transfer rate. Thermal conductivity, on the other hand, refers to the ability of the material to conduct heat, and it can also affect the heat transfer rate in the system. By considering these factors, this work provides a more realistic and accurate representation of the thermos-physical properties of the system.

The purpose of this research work is to investigate the significance of temperature-dependent viscosity and temperature-dependent thermal conductivity on the work of Ekang *et al.* (2021). The obtained ordinary differential equations are solved numerically using shooting method along with fourth-order Runge-Kutta method. The effects of various fluid parameters on the momentum, thermal and concentration profiles are considered and exhibited graphically.

2. Materials and Methods

We consider a two-dimensional, steady flow of an incompressible nano-fluid exhibiting MHD heat and mass transfer. The flow occurs over a non-linear permeable stretching sheet aligned with the $y = 0$ plane. The coordinate system measures the distance normal to the surface of the stretching sheet in the vertical direction $y \geq 0$.

The flow is induced by a sheet emerging from a slit located at the origin $(x = y = 0)$. The stretching velocity, denoted as u_w, varies nonlinearly with the distance from the slit. The non-linear variation is described by the equation $u_w = ax^n$, where a > 0, n represents the non-linear stretching parameter, and x is the coordinate measured along the surface.

The sheet's surface is exposed to a specified temperature, which is expressed as follows:

$T = T_\infty + b_1 x^r$ at y = 0 (1)

where $b_1 > 0$, r be the temperature parameter at the surface in the boundary condition, T_∞

represents the ambient temperature, T_w is the temperature at the surface. Additionally, the surface is held at a constant concentration, C_w, with its value assumed to be higher than the ambient concentration, C_∞, given as:

$$C = C_\infty + (C_w - C_\infty) \text{ at y = 0} \quad (2)$$

The mathematical model of the temperature-dependent viscosity and temperature-dependent thermal conductivity is taken into account in the analysis:

$\mu(T) = \mu^*(1 + b(T - T_\infty))$ and $k(T) = k^*(1 + \delta(T - T_\infty))$ (3)

with $b, \delta > 0$.

We assumed a uniform magnetic field with strength B_o applied perpendicular to the stretching sheet at y > 0. Under this condition, the governing equations are as follows:

$$\frac{\partial u}{\partial x} + \frac{\partial v}{\partial y} = 0 \quad (4)$$

$$u\frac{\partial u}{\partial x} + v\frac{\partial u}{\partial y} = \frac{1}{\rho}\left(\frac{\partial}{\partial x}\left(\mu(T)\frac{\partial u}{\partial y}\right) + \frac{\partial}{\partial y}\left(\mu(T)\frac{\partial u}{\partial y}\right)\right) - \frac{\sigma B_0^2}{\rho}u - \frac{\mu(T)}{\rho K}u \quad (5)$$

$$u\frac{\partial T}{\partial x} + v\frac{\partial T}{\partial y} = \frac{1}{\rho C_p}\left[\frac{\partial}{\partial x}\left(k(T)\frac{\partial T}{\partial x}\right) + \frac{\partial}{\partial y}\left(k(T)\frac{\partial T}{\partial y}\right)\right] + \tau\left[\mathrm{D}_B\left(\frac{\partial C}{\partial x}\frac{\partial T}{\partial x} + \frac{\partial C}{\partial y}\frac{\partial T}{\partial y}\right) + \left(\frac{\mathrm{D}_T}{T_\infty}\right)\left\{\left(\frac{\partial T}{\partial x}\right)^2 + \left(\frac{\partial T}{\partial y}\right)^2\right\}\right] \quad (6)$$

$$u\frac{\partial C}{\partial x} + v\frac{\partial C}{\partial y} = \mathrm{D}_B\left(\frac{\partial^2 C}{\partial x^2} + \frac{\partial^2 C}{\partial y^2}\right) + \left(\frac{\mathrm{D}_T}{T_\infty}\right)\left(\frac{\partial^2 T}{\partial x^2} + \frac{\partial^2 T}{\partial y^2}\right) \quad (7)$$

The corresponding boundary conditions are as follows:

$$u = u_w + u_s,\ v = \pm v_w,\ T = T_w,\ C = C_w \text{ at } y = 0$$
$$u \to 0,\ T \to T_\infty,\ C \to C_\infty \text{ as } y \to \infty \quad (8)$$

In equations (4) – (8), the variables u and v represent the velocity components along the x- and y- axes, respectively. The symbol $\vartheta = \frac{\mu}{\rho}$ denotes the kinematic viscosity, ($\frac{\mu}{\rho}$), where μ is the dynamic viscosity and ρ is the fluid density. The parameter σ represents the electrical conductivity, K represents the constant permeability of the porous medium and α is the thermal diffusivity where k is the thermal conductivity and c_p is the specific heat capacity.

The term τ represents the ratio between the effective heat capacity of the nano-particle material and heat capacity of the fluid, given by $\frac{(\rho c)_p}{(\rho c)_f}$. The symbol c corresponds to the volumetric volume expansion coefficient, ρ_f represents the density of the base fluid, D_T is the thermophoretic diffusion coefficient, and D_B is the Brownian diffusion coefficient.

Furthermore, v_w denotes the suction/ injection velocity and u_s is the slip velocity which is assumed to be proportional to the local wall stress.

$$u_s = l\left(\frac{\partial u}{\partial x} + \frac{\partial u}{\partial y}\right)\Big|_{y=0} \quad (9)$$

The slip length, denoted by l , serves as proportional constant for the slip velocity.

The transformation below is used to convert equations (5) – (7) into non-dimensional ordinary differential equations:

$$\psi = \left(\frac{2\vartheta a x^{n+1}}{n+1}\right) f(\eta),\ \eta = \left(\frac{a(n+1)x^{n-1}}{2\vartheta}\right)^{1/2} y,$$
$$u = a x^n f'(\eta)$$
$$v = -\left(\frac{\vartheta a(n+1)x^{n-1}}{2}\right)^{1/2}\left[f + \frac{(n-1)}{(n+1)}\eta f'\right],$$
$$T = T_\infty + b_1 x^r \theta(\eta),\quad \phi(\eta) = \frac{C - C_\infty}{C_w - C_\infty}$$

where ψ is the stream function defined as:

$$u = \frac{\partial \psi}{\partial y},\quad v = -\frac{\partial \psi}{\partial x}$$

The resulting transformed ordinary differential equations are given by:

$$[1 + E\theta]\left[\frac{[2Re(n+1) + (n-1)^2\eta^2]}{2Re(n+1)}\right] f''' + ff'' + \frac{(n-1)(5n-3)}{2(n+1)}\frac{1}{Re}\eta f'' - \frac{2n}{n+1}f'^2 + \frac{n(n-1)}{n+1}\frac{E}{Re}\eta\theta' f' + \frac{(n-1)(5n+2r-3)}{2(n+1)}\frac{E}{Re}\eta\theta f'' +$$

$$E\left[\frac{2Re(n+1)+(n-1)^2\eta^2}{2Re(n+1)}\right]\theta' f'' + \frac{2}{n+1}\left[\frac{n(2n+r-2)}{Re}(1+E\theta) - Ha - La(1+E\theta)\right]f' = 0 \quad (10)$$

$$[1+F\theta]\left[\frac{(n-1)^2\eta^2+2(n+1)Re}{4}\right]\frac{1}{p_r}\theta'' + \frac{n+1}{2}Ref\theta' - rRef'\theta + r[(r-1)+(2r-1)F\theta]\frac{1}{p_r}\theta + \left[\frac{1}{2}+F\theta\right]\frac{1}{p_r}(n-1)r\eta\theta' + [(n+2r-3)+(n+4r-3)F\theta]\frac{n-1}{4}\frac{1}{p_r}\eta\theta' + F\frac{1}{p_r}\left[\frac{(n-1)^2\eta^2+2(n+1)Re}{4}\right]\theta'^2 + \frac{n-1}{2}rNb\eta\phi'\theta + r^2Nt\theta^2 + (n-1)rNt\eta\theta\theta' + \left[\frac{(n-1)^2\eta^2+2(n+1)Re}{4}\right]Nb\phi'\theta' + \left[\frac{(n-1)^2\eta^2+2(n+1)Re}{4}\right]Nt\theta'^2 = 0 \quad (11)$$

$$\left[\frac{(n-1)^2\eta^2+2(n+1)Re}{4}\right]\phi'' + \frac{n+1}{2}Lef\phi' + \frac{(n-1)(n-3)}{4}\eta\phi' + r(r-1)\frac{Nt}{Nb}\theta + \frac{(n-1)(n+4r-3)}{4}\frac{Nt}{Nb}\eta\theta' + \left[\frac{(n-1)^2\eta^2+2(n+1)Re}{4}\right]\frac{Nt}{Nb}\theta'' = 0 \quad (12)$$

Subject to the following boundary conditions:

$$f(\eta) = f_w, \quad f'(\eta) = 1+\beta f''(\eta), \quad \theta(\eta) = 1, \quad \phi(\eta) = 1 \quad \text{at} \quad \eta = 0$$

$$f'(\eta) \to 0, \theta(\eta) \to 0, \phi(\eta) \to 0 \text{ as } \eta \to \infty \quad (13)$$

The given variables are defined as follows: $Re = \frac{xu_w}{\vartheta}$ is the Reynolds number, $Ha = \frac{x\sigma B_0^2}{u_w\rho}$ is the Magnetic parameter, $La = \frac{x\vartheta}{u_wK}$ is the Permeability parameter, $\Pr = \frac{\vartheta}{\alpha}$ is the Prandtl number, $Le = \frac{u_wx}{D_B}$ is the Lewis number, $Nb = \frac{\tau D_B(C_w-C_\infty)}{\vartheta}$ is the Brownian motion parameter, $E = bb_1x^r$ is the temperature-dependent viscosity, $F = \delta b_1x^r$ is the temperature-dependent thermal conductivity, $Nt = \frac{\tau D_T b_1 x^r}{\vartheta T_\infty}$ is the thermophoresis parameter, $f_w = -\frac{v_w}{(\frac{a\vartheta(n+1)x^{n-1}}{2})^{1/2}}$ is the suction/ injection parameter, and $\beta = l(\frac{a(n+1)x^{n-1}}{2\vartheta})^{1/2}$ is the slip parameter for liquids.

The skin friction coefficient, C_f, the local Nusselt number, Nu_x, and the Sherwood number, Sh_x, are the primary physical quantities of interest. These quantities are defined as follows:

$$C_f = \frac{\tau_w}{\rho u_w^2}, Nu_x = \frac{xq_w}{k_1(T_w-T_\infty)}, Sh_x = \frac{xJ_w}{D_B(C_w-C_\infty)} \quad (14)$$

And for which $\tau_w = \mu(\frac{\partial u}{\partial y})_{y=0}$ is the surface shear stress, $q_w = -k(\frac{\partial T}{\partial y})_{y=0}$ is the heat flux, $J_w = -D_B(\frac{\partial C}{\partial y})_{y=0}$ is the wall mass flux, μ is the dynamic viscosity and k is the thermal conductivity. Through the utilization of similarity variables, we can express these as:

$$Re_x^{1/2}C_f = (\frac{n+1}{2})^{1/2}f''(0), Re_x^{-1/2}Nu_x = -(\frac{n+1}{2})^{1/2}\theta'(0), \quad Re_x^{-1/2}Sh_x = -(\frac{n+1}{2})^{1/2}\phi'(0) \quad (15)$$

To solve the dimensionless governing equations (10), (11) and (12) with their corresponding boundary conditions (13), we employ the shooting method in combination with the fourth order Runge-Kutta technique. Initially, we introduce new variables for the equations as follows:

$$f_1 = \eta, \ f_2 = f, \ f_3 = f', \ f_4 = f'', \ f_5 = \theta, \ f_6 = \theta', f_7 = \phi, f_8 = \phi' \quad (16)$$

The coupled higher order non-linear differential equations (10), (11), and (12) along with the boundary conditions (13), which govern the system in the dimensionless form, are converted into a system of first order differential equations. In accordance with standard practice in the boundary layer analysis, the boundary conditions are modified by replacing the conditions as $\eta \to \infty$ with a finite value.

$$f_1' = 1$$
$$f_2' = f_3$$
$$f_3' = f_4$$
$$f_4' = (\frac{2Re(n+1)}{[1+E\theta][2Re(n+1)+(n-1)^2\eta^2]})(-ff'' - \frac{(n-1)(5n-3)}{2(n+1)}\frac{1}{Re}\eta f'' + \frac{2n}{n+1}f'^2 - \frac{n(n-1)}{n+1}\frac{E}{Re}\eta\theta' f' - \frac{(n-1)(5n+2r-3)}{2(n+1)}\frac{E}{Re}\eta\theta f'' - E\left[\frac{2Re(n+1)+(n-1)^2\eta^2}{2Re(n+1)}\right]\theta' f'' - \frac{2}{n+1}\left[\frac{n(2n+r-2)}{Re}(1+E\theta) - Ha - La(1+E\theta)\right]f')$$

$$f_5' = f_6 \qquad (17)$$

$$f_6' = \left(\frac{4Pr}{[1+F\theta][(n-1)^2\eta^2+2(n+1)Re]}\right)\left(-\frac{n+1}{2}Ref\theta' + rRef' - r[(r-1)+(2r-1)F\theta]\frac{1}{p_r}\theta - \left[\frac{1}{2}+F\theta\right]\frac{1}{p_r}(n-1)r\eta\theta' - [(n+2r-3) + (n+4r-3)F\theta]\frac{n-1}{4}\frac{1}{p_r}\eta\theta' - F\frac{1}{p_r}\left[\frac{(n-1)^2\eta^2+2(n+1)Re}{4}\right]\theta'^2 - \frac{n-1}{2}rNb\eta\phi'\theta - r^2Nt\theta^2 - (n-1)rNt\eta\theta\theta' - \left[\frac{(n-1)^2\eta^2+2(n+1)Re}{4}\right]Nb\phi'\theta' - \left[\frac{(n-1)^2\eta^2+2(n+1)Re}{4}\right]Nt\theta'^2\right)$$

$$f_7' = f_8$$

$$f_8' = \left(\frac{4}{(n-1)^2\eta^2+2(n+1)Re}\right)\left(-\frac{n+1}{2}Lef\phi' - \frac{(n-1)(n-3)}{4}\eta\phi' - r(r-1)\frac{Nt}{Nb}\theta - \frac{(n-1)(n+4r-3)}{4}\frac{Nt}{Nb}\eta\theta' - \left[\frac{(n-1)^2\eta^2+2(n+1)Re}{4}\right]\frac{Nt}{Nb}\theta'^2\right)$$

In the analysis, the notation of primes represents differentiation with respect to η. Initially, we make educated guesses for the values of $f''(0)$, $\theta'(0)$, and $\phi'(0)$ to ensure equation (13) is satisfied. The obtained results are then presented through tables, graphs, and subsequently analysed and discussed to highlight their key features.

3. Results and Discussion

The significant effects of fluid factors such as temperature-dependent viscosity, temperature-dependent thermal conductivity, nonlinear stretching parameter, magnetic field parameter, permeability parameter, Brownian motion parameter, thermophoresis parameter, Prandtl number, Lewis number on velocity, temperature and nano-particle concentration profiles are analysed numerically using the shooting method. Numerical values obtained were plotted into graphs varying the fluid parameters with basic at $r = 1$, $n = 2$, $f_w = 0.2$, $Re = 1$, $Ha = 1$, $La = 1$, $Le = 5$, $Nb = 0.5$, $Nt = 0.5$, $Pr = 2$, $E = 1$, $F = 1$.

The influence of temperature-dependent viscosity on the $f'(\eta)$, $\theta(\eta)$, $\phi(\eta)$ are shown in Figs. 1, 2, 3. An increase in temperature-dependent viscosity led to an increase in the $f'(\eta)$ of the fluid. As the temperature of the fluid increased, the viscosity decreased, which in turn led to a decrease in the internal friction of the fluid. As a result, the fluid flew more easily and at a higher velocity.

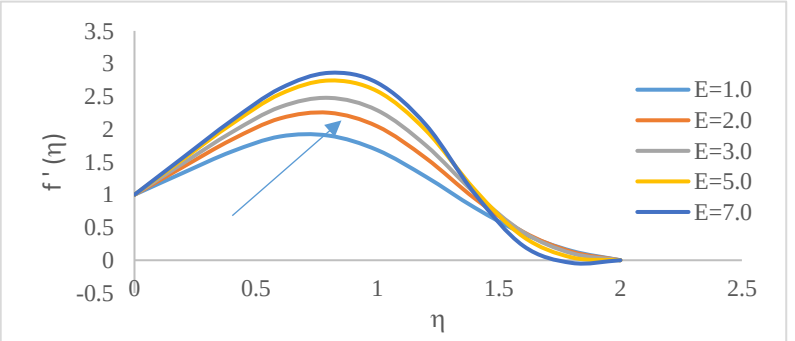

Figure 1. Varying of E on velocity profiles

An increase in the values of temperature-dependent viscosity had significant impact on the temperature profiles. Viscosity of the fluid changes with temperature, which affect the flow behaviour of the fluid. A higher viscosity impedes

the flow of heat through the fluid which result in a lower temperature gradient.

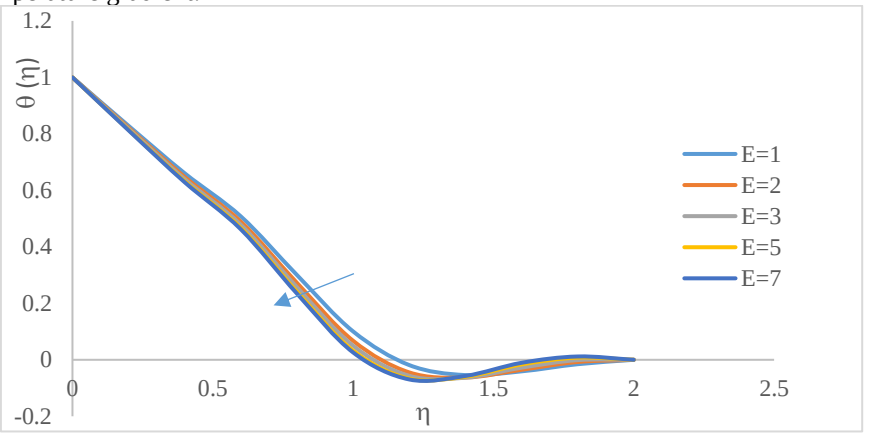

Figure 2. Varying of E on temperature profiles

An increase in the temperature-dependent viscosity led to an increase in the concentration profiles of nano-particles. The increase in the viscosity resulted in a higher drag force on the Nano-particles, which caused them to accumulate near the stretching surface. This effect was enhanced when the temperature-dependent viscosity was considered since an increase in temperature led to a decrease in viscosity and subsequently lower drag force on the nano-particles and the concentration of the nano-particles in the fluid increased.

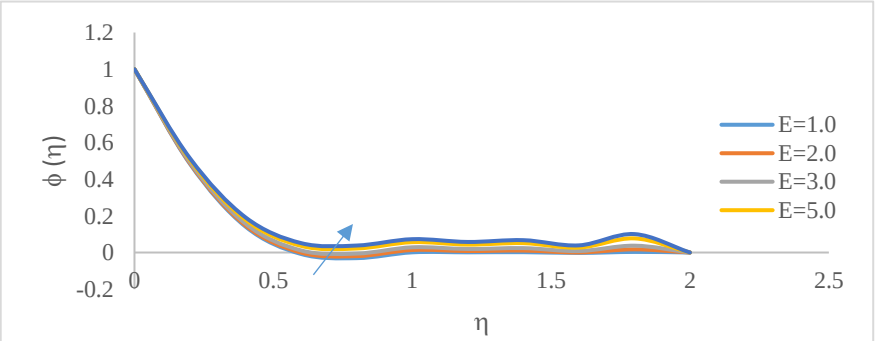

Figure 3. Varying of E on concentration profiles

Figs. 4, 5 and 6 show the effect of temperature-dependent thermal conductivity on the $f'(\eta)$, $\theta(\eta)$, $\phi(\eta)$of the fluid. An increase in temperature-dependent thermal conductivity has an impact on the velocity profiles. As the thermal conductivity of the fluid increases with temperature, the heat transfer rate through the fluid also increases. This leads to a temperature gradient across the fluid, which in turn create thermal buoyancy forces that affect the fluid flow behaviour.

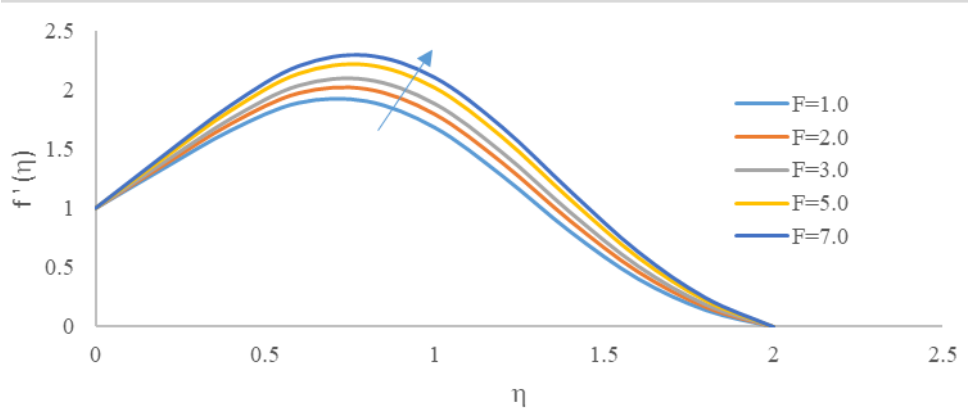

Figure 4. Varying of F on velocity profiles

An increase in temperature-dependent thermal conductivity has a significant impact on the temperature profiles. The thermal conductivity of the fluid changes with temperature which affect the flow behaviour of the fluid. A higher thermal conductivity enhances the flow of heat through the fluid which result in a higher temperature gradient.

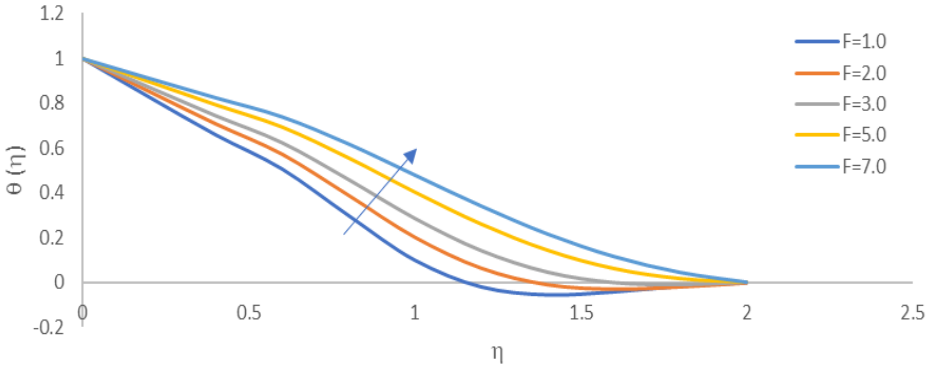

Figure 5. Varying of F on temperature profiles

An increase in temperature-dependent thermal conductivity leads to a decrease in the concentration profiles of nano-particles. The decrease in the concentration of nano-particles is attributed to the phenomenon of Brownian motion. As the temperature of the fluid increases, the fluid molecules become more energetic leading to an increase in the rate of Brownian motion. The nano-particles in the fluid collide with the fluid molecules and become dispersed throughout the fluid leading to a decrease in their concentration near the stretching surface.

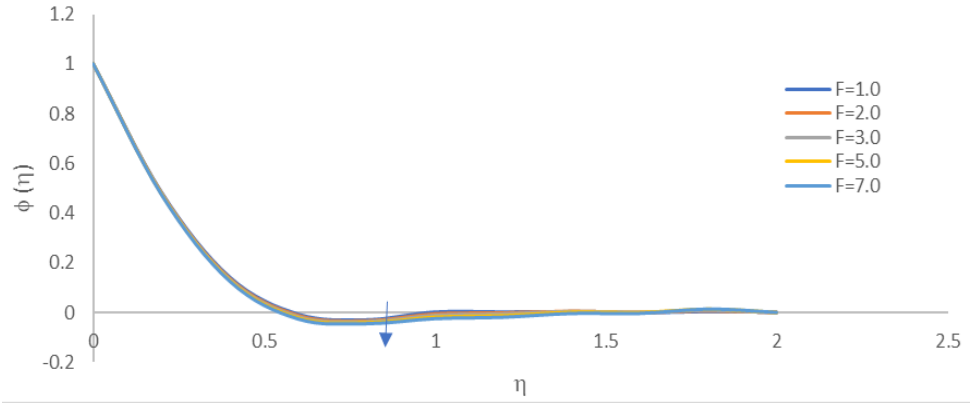

Figure 6. Varying of F on nano-particle concentration profiles

Figs. 7, 8, 9 depict the effect of the nonlinear stretching parameter on the $f'(\eta)$, $\theta(\eta)$, $\phi(\eta)$of the fluid. An increase in the values of the nonlinear stretching parameter also affect the velocity profiles. The stretching parameter describes the degree of nonlinearity in the stretching of the sheet and a larger stretching parameter implies a more significant stretching effect which in turn cause the fluid to accelerate and flow faster.

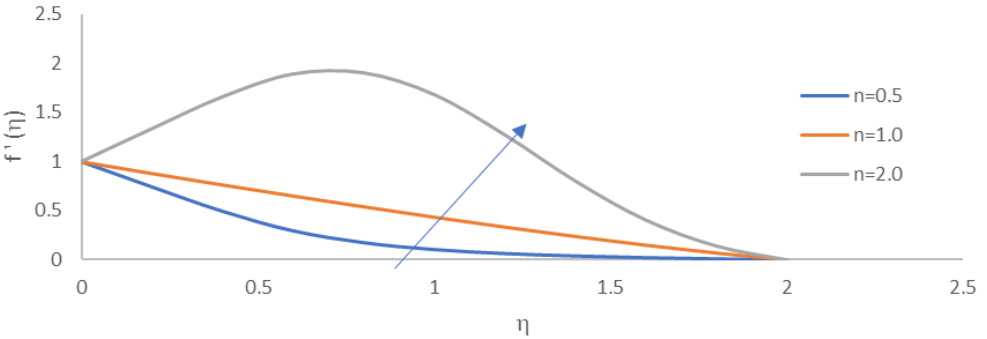

Figure 7. Varying of n on Velocity profiles

An increase in the values of the nonlinear stretching parameter have a significant impact on the temperature profiles. The stretching parameter describes the degree of stretching applied to the fluid which affect the flow behaviour of the fluid and also results in decrease of temperature distribution in the system.

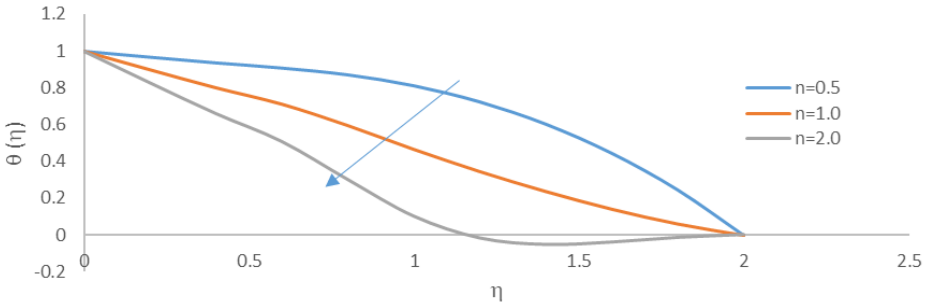

Figure 8. Varying of n on Temperature profiles

An increase in the nonlinear stretching leads to a decrease in the concentration profiles of nano-particles. The nonlinear stretching parameter describes the rate at which the stretching surface increases in size along a particular direction. An increase in the nonlinear stretching parameter results in a faster increase in the size of the stretching surface, which in turn lead to a decrease in the concentration of nano-particles in the fluid near the stretching surface.

As the stretching surface expands rapidly, the fluid molecules near the surface experience a rapid increase in temperature, leading to a significant temperature gradient. This temperature gradient causes the nano-particles to move away from the stretching surface in response to thermophoresis. However, the random motion of the particles due to Brownian motion causes them to diffuse back towards the stretching surface. The time available for the particles to diffuse back towards the surface decreases, leading to a decrease in the concentration of nano-particles near the surface.

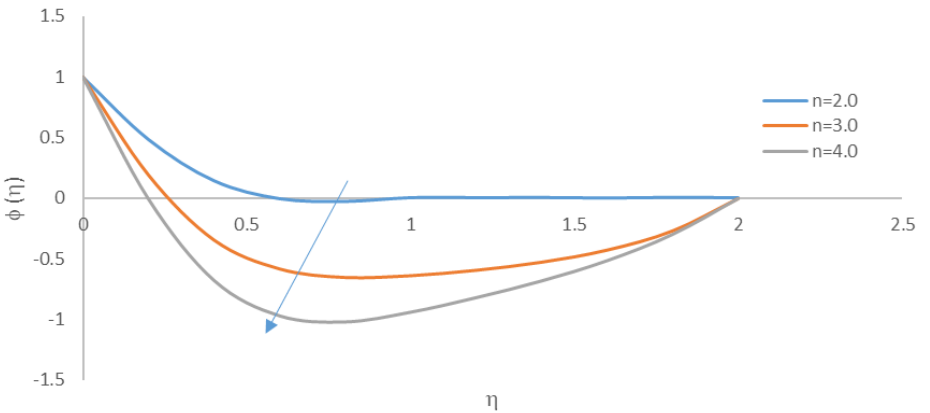

Figure 9. Varying of n on nano-particle concentration profiles

Figs. 10 and 11 show how the $f'(\eta)$ and $\theta(\eta)$ of the fluid are affected by the magnetic field parameter. An increase in the values of magnetic field parameter affect the velocity profiles. The magnetic field parameter describes the strength of the applied magnetic field, and a larger magnetic field parameter implies a stronger magnetic field affect. A stronger magnetic field generate a magnetic Lorentz force that oppose the fluid motion leading to a reduction in velocity profiles.

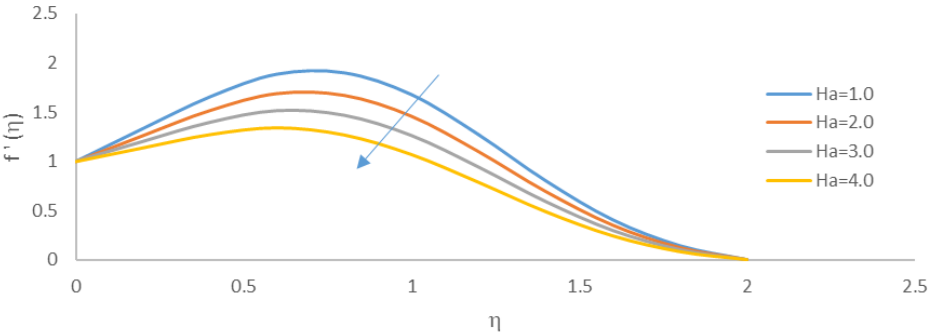

Figure 10. Varying of Ha on velocity profiles

An increase in the values of the magnetic field has a significant impact on the temperature profiles. The magnetic field parameter describes the strength of the applied magnetic field which affect the flow behaviour of the fluid and the distribution of temperature in the system. A higher magnetic field enhance the conduction of heat through the fluid which results in a higher temperature gradient.

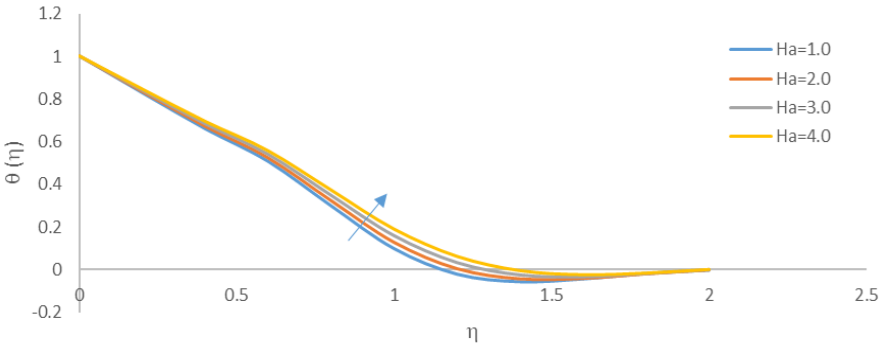

Figure 11. Varying of Ha on temperature profiles

Figs. 12 and 13 illustrate how the permeability parameter affects the $f'(\eta)$ and $\theta(\eta)$ of the fluid. An increase in the values of the permeability parameter can also affect the velocity profiles. The permeability parameter describes the degree of permeability of the stretching sheet, and a larger permeability implies a higher degree of permeability which increases the drag force on the fluid and in turn reduce the fluid velocity.

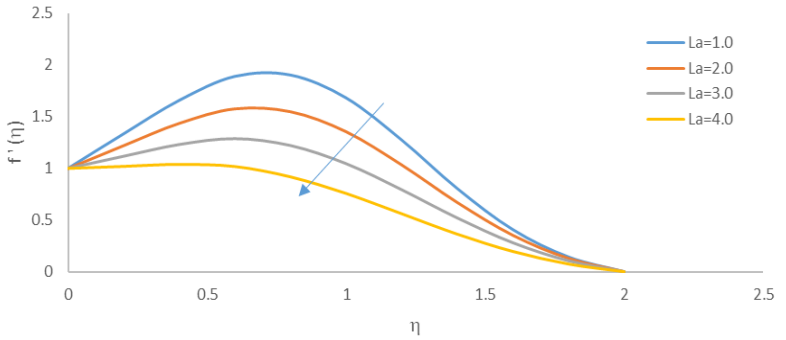

Figure 12. Varying of La on velocity profiles

An increase in the values of permeability parameter has a significant impact on the temperature profiles. The permeability parameter describes the degree of permeability of the stretching sheet, which affect the flow behaviour of the fluid and the distribution of temperature in the system. A higher permeability results in a higher rate of heat transfer from the stretching sheet to the fluid which lead to a higher temperature gradient in the system.

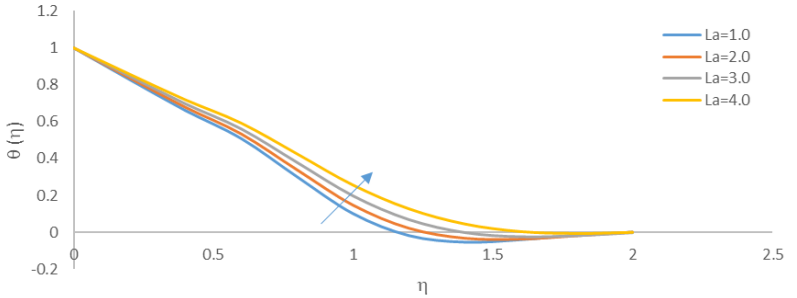

Figure 13. Varying of La on temperature profiles

Figs. 14 and 15 depicts how the $f'(\eta)$ and $\theta(\eta)$ is affected by the Brownian motion parameter of the fluid. An increase in the values of the Brownian motion parameter affect the velocity profiles. The Brownian motion parameter describes the degree of Brownian motion of the nano-particles suspended in the fluid and a higher degree of Brownian motion leads to an increased collision frequency between the nano-particles and the fluid, which in turn enhance the fluid velocity.

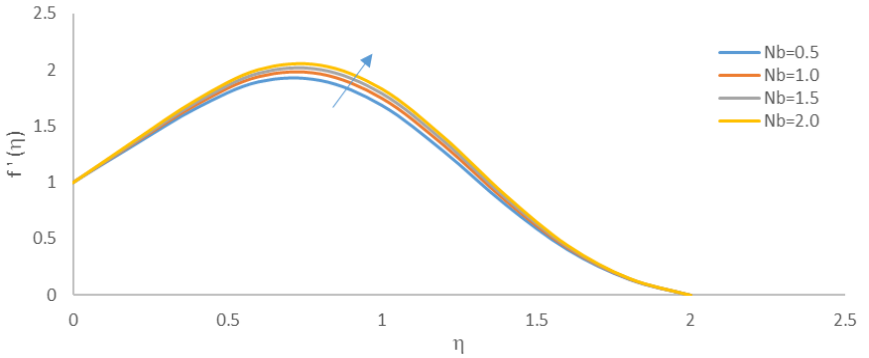

Figure 14. Varying of Nb on velocity profiles

The Brownian motion parameter represents the effect of random thermal motion on the nano-particles suspended in the base fluid. An increase in the Brownian motion parameters result in an increase in the random motion of the nano-particles which leads to an increase in their collision frequency with the fluid molecules. This increased frequency result in enhanced heat transfer between the nano-particles and the fluid, leading to an increase in the temperature profiles. An increase in the Brownian motion parameters result in an increase in the effective thermal conductivity of the nano-particles fluid mixture, as the enhanced nano-particle motion leads to better mixing of the fluid and the nano-particles. This increased effective thermal conductivity further enhances the heat transfer between the nano-particles and the fluid leading to an increase in the temperature profiles.

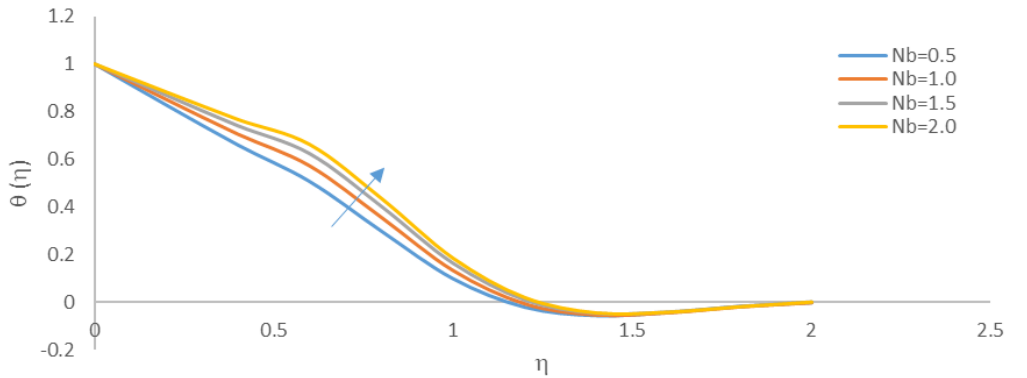

Figure 15. Varying of Nb on temperature profiles

Figs. 16, 17 and 18 highlight the effect of thermophoresis parameter on the $f'(\eta)$, $\theta(\eta)$, $\phi(\eta)$ of the fluid. An increase in the values of the thermophoresis parameter affect the velocity profiles. The thermophoresis parameter describes the degree of thermophoresis of the nano-particles suspended in the fluid and a higher degree of thermophoresis leads to an increased mass flux of the nano-particles towards the stretching sheet which in turn enhance the fluid velocity.

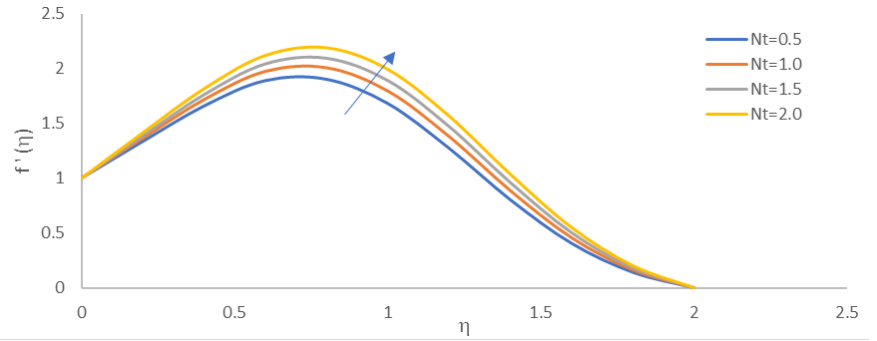

Figure 16. Varying of Nt on velocity profiles

It is observed that the temperature increases with increasing values of thermophoresis parameters. Thermophoresis parameter increases the thermal boundary layer thickness and the temperature on the surface of the sheet increases. This is because the thermophoresis parameter is directly proportional to the heat transfer coefficient associated with the fluid.

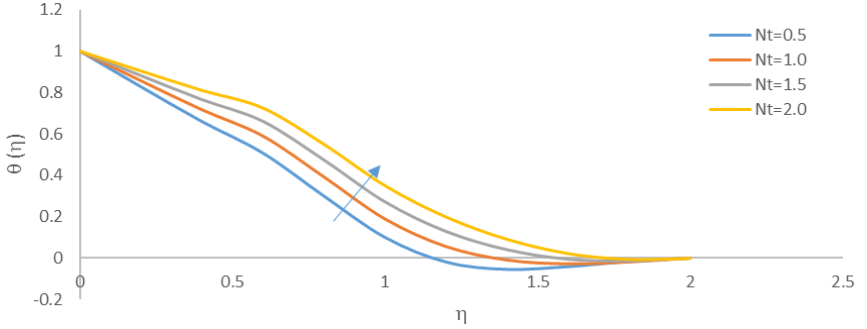

Figure 17. Varying of Nt on temperature profiles

The concentration profiles decrease with increasing values of thermophoresis parameters. Concentration is a decreasing function of thermophoresis parameter. For hot surfaces, thermophoresis tends to blow the nano-particle volume fraction boundary layer away from the surface since hot surface repels the submicron-sized particles from it, thereby forming a relatively particle-free layer near the surface.

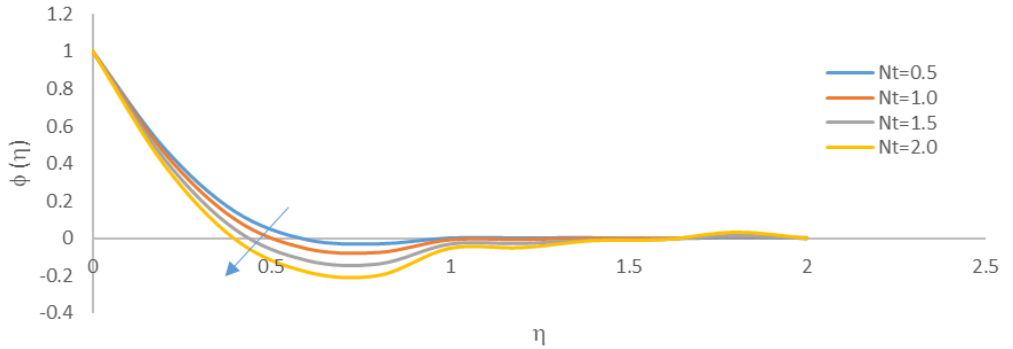

Figure 18. Varying of Nt on nano-particle concentration profiles

Figs. 19 and 20 represents the $f'(\eta)$ and $\theta(\eta)$, for various values of Prandtl numbers of the fluid. An increase in the Prandtl numbers leads to a decrease in velocity profiles. A higher Prandtl number implies that the fluid has a higher viscosity relative to its thermal conductivity which dampen the fluid velocity. This is because a higher viscosity can resist the flow of the fluid whereas a higher thermal conductivity enhances the transfer of heat through the fluid.

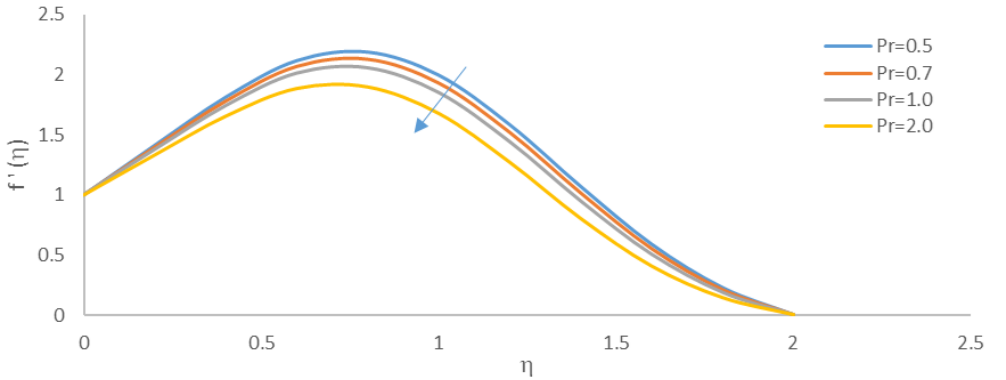

Figure 19. Varying of Pr on velocity profiles

An increase in the Prandtl numbers corresponds to an increase in the ratio of thermal diffusivity to momentum diffusivity, indicating that the fluid is less efficient at transferring heat compared to momentum. A higher Prandtl number signifies that the fluid is less efficient at transferring heat, which result in a lower temperature gradient in the system.

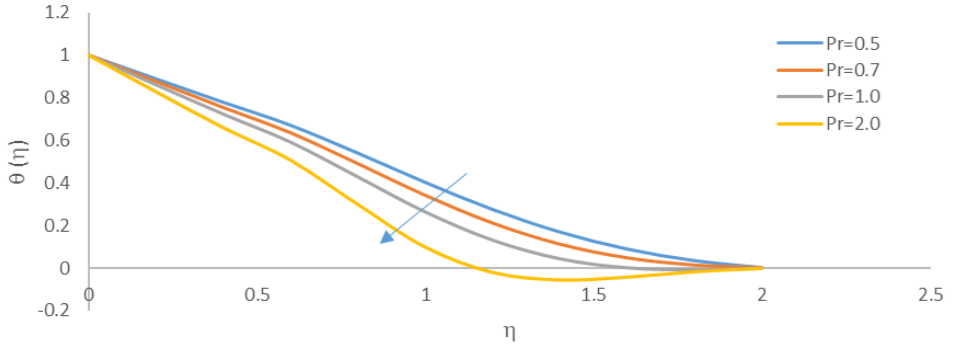

Figure 20. Varying of Pr on temperature profiles

Fig. 21 manifest the Lewis number on the $\phi(\eta)$ of the fluid. A higher Lewis number indicates that thermal diffusivity is greater than mass diffusivity which implies that the rate of heat transfer in the fluid is higher compared to the rate of mass transfer. As a result, the temperature of the fluid increases faster than the concentration of the nano-particles leading to a decrease in the concentration profiles of the nano-particles. Thermal energy in the fluid is transferred more easily than the nano-particles due to the difference in their diffusivities.

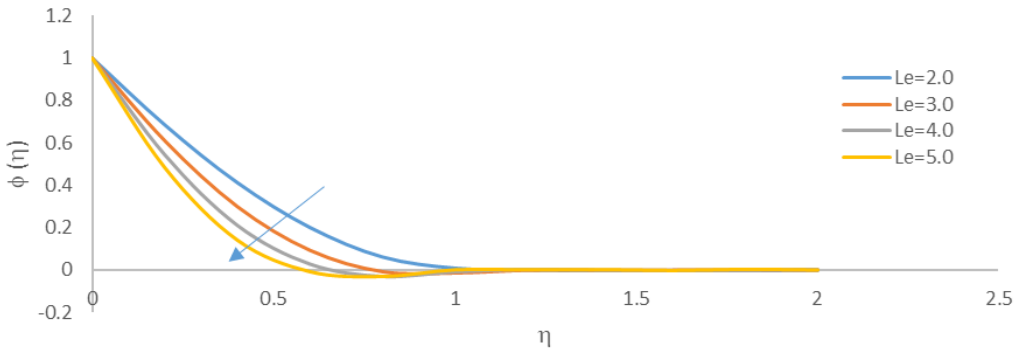

Figure 21. Varying of Le on nano-particle concentration profiles

Table 1. The numerical values of $f''(0)$, $\theta'(0)$, $\phi'(0)$ for different values of temperature-dependent viscosity, E.

E	$f''(0)$	$\theta'(0)$	$\phi'(0)$
1.0	1.51940	-0.77990	-2.35010
2.0	1.92866	-0.80970	-2.33274
3.0	2.18075	-0.82658	-2.30530
5.0	2.46402	-0.84498	-2.24707
7.0	2.58328	-0.85274	-2.21220

Table 1 represents values of skin-friction coefficient, Nusselt number and Sherwood number for various values of temperature-dependent viscosity. It shows that an increase in the values of temperature-dependent viscosity increases skin-friction coefficient and Sherwood number while the Nusselt number decreases.

Table 2: The numerical values of $f''(0)$, $\theta'(0)$, $\phi'(0)$ for different values of temperature-dependent thermal conductivity, F.

F	$f''(0)$	$\theta'(0)$	$\phi'(0)$
1.0	1.51940	-0.77990	-2.35010
2.0	1.64856	-0.66447	-2.36230
3.0	1.75190	-0.58200	-2.36990
5.0	1.90390	-0.46961	-2.38360
7.0	2.00550	-0.39810	-2.39440

Table 2 represents values of skin-friction coefficient, Nusselt number and Sherwood number for various values of temperature-dependent thermal conductivity. It shows that an increase in the values of temperature-dependent thermal conductivity increases skin-friction coefficient and Nusselt number while the Sherwood number decreases.

4. Conclusion

The effects of the fluid parameters on the flow and heat transfer are examined with the help of graphs and are summarized as follows:

- An increase in temperature-dependent viscosity enhances the velocity and nano-particle concentration profiles while the temperature profiles decrease.
- The velocity and temperature profiles are increasing functions of temperature-dependent thermal conductivity whereas the nano-particle concentration profiles are decreasing function.
- An increase in the nonlinear stretching parameters enhances velocity profiles and reduces that of the temperature and nano-particle concentration profiles.
- The velocity profiles decrease with increasing values of magnetic field and permeability parameters while the temperature profiles increase.
- An increase in the Brownian motion parameters enhances velocity and temperature profiles.
- An increase in the thermophoresis parameters leads to an increase in the velocity and temperature profiles but reduces the nano-particle concentration profiles.
- Increasing the Prandtl numbers reduces the velocity and temperature profiles.
- The nano-particle concentration profiles are decreasing function of Lewis number.

Conflict of Interest

We declare that there is no conflict of interest.

Orcid
Idongesit Fred Ekang https://orcid.org/0000-0002-4014-7635
Amos Oladele Popoola https://orcid.org/0000-0002-3376-9938

Reference

Ayeni, R. O., Popoola, A. O., Omowaye, A. J. and Ayeni, O. B. (2009). MHD flow and heat transfer of a viscous reacting fluid over a stretching sheet, *Journal of the Nigerian Association of Mathematical Physics*, 15(1), 485-490.

Crane, L. J. (1970). Flow past a stretching plate, *Z. Angew. Math. Phys*., 21,645-647.

Das, K. (2015). Nanofluid flow over a nonlinear permeable stretching sheet with partial slip, *Journal of the Egyptian Mathematical Society*, 23,451-456.

Eid, M. R., and Mahny, K. L. (2017). Unsteady MHD heat and mass transfer of a non-Newtonian nanofluid flow of a two-phase Model over a permeable stretching wall with heat generation/absorption, *Advanced Powder Tech.*, in press, doi: 10.1016/j.apt.2017.09.021.

Ekang, I. F., Joshua, E. E. and Senge, I. O. (2022). Casson fluid flow with heat generation and radiation effect through a porous medium of an exponentially shrinking sheet. *World Journal of Applied Science and Technology*,14(1b), 56-61. doi.org/10.4314/WOJAST.v14i1b.56.

Ekang, I. F., Joshua, E. E., Senge, I. O. and Nwachukwu, O. O. (2021). MHD heat and mass flow of nano-fluid over a non-linear permeable stretching sheet, *Journal of Mathematics and Computational Science*, 11(5), 5196- 5212.

Gupta, P. S. and Gupta, A. S. (1977). Heat and mass transfer on a stretching sheet with suction or blowing, *Canad. J. Chem. Eng.*, 55,744-746.

Khan, W. A. and Pop, I. (2010). Boundary layer flow of a nanofluid past a stretching sheet, *International Journal Heat Mass Transfer*, 53,2477-2483.

Oreyeni, T., Ramesh, K., Nayak, M. K. and Popoola, A. O. (2022). Triple stratification impacts on an inclined hydromagnetic bioconvective flow of micropolar nanofluid with exponential space-based heat generation, *Waves in Random and Complex Media*, doi: 10.1080/17455030.2022.2112994.

Oreyeni, T., Shah, N. A. and Popoola, A. O. (2022). The significance of exponential space-based heat generation and variable thermophysical properties on the dynamics of Casson fluid over a stratified surface with non-uniform thickness, *Waves in Random and Complex Media*, doi: 10.1080/17455030.2022.2119304.

Popoola, A. O., Baoku, I. G. and Olajuwon, B. I. (2016). Heat and mass transfer on MHD viscoelastic fluid flow in the presence of thermal diffusion and chemical reaction, *International Journal of Heat and Technology*, 34(1), 15-26.

Rana, P. and Bhargava, R. (2012). Flow and heat transfer of a nanofluid over a nonlinearly stretching sheet: a numerical study, *Commun. Nonlinear Sci. Numer. Simul.*, 17,212-226.

Sakiadis, B. C. (1961). Boundary layer behaviour on continuous solid surfaces, *AIChEJ*., 7,26-28.

Senge, I. O., Oghre, E. O. and Ekang, I. F. (2021). Influence of radiation on magneto-hydrodynamics flow over an exponentially stretching sheet embedded in a thermally stratified porous medium in the presence of heat source, *Earthline Journal of Mathematical Sciences*, 5,2,345-363.

Vajravelu, K. (2001). Viscous flow over a nonlinearly stretching sheet, *App. Math. Comput.*,124,281-288.

Wang, C. Y. (2009). Analysis of viscous flow due to a stretching sheet with surface slip and suction, *Nonlinear Anal. Real. World Appl.*, 10,375-380.